# MULTIANODE GAS COUNTER FOR LOW INTENSITY BEAM DIAGNOSTICS AT THE INR LINAC

A. Melnikov[†], S. Gavrilov,

Institute for Nuclear Research of the Russian Academy of Sciences, Troitsk, Moscow, Russia and Moscow Institute of Physics and Technology (State University), Moscow, Russia

## Abstract

Multianode gas counter is used to measure beam intensity in ionization mode and profiles in proportional mode at a new INR RAS proton irradiation facility. A special model is created in COMSOL to simulate operational characteristics of this counter. A program for data acquisition and processing is based on LabVIEW. Operational characteristics of the counter and experimental results of beam measurements are presented. Upgrade of the existing software and hardware is discussed.

## INTRODUCTION

A proton irradiation facility (PIF) at INR RAS linac is used to study radiation effects in electronic components. This facility is characterized with working parameters: proton energy - 20÷210 MeV; particles per pulse - $10^7 \div 10^{12}$; pulse duration - 0.3÷180 μs; pulse repetition rate - 1÷50 Hz.

Partially diagnostics was realized with a beam current transformer (BCT) installed in the beam pipe. It provides absolute nondestructive measurements of beam pulse current with the amplitude > 25 μA. The BCT is not applicable for less intensive beams and for measurement of beam profiles. In this case induced field detectors do not work. Detectors based on gas ionization are widely used for low intensity beams. One of the ways to measure beam current and profiles is to collect ionization particles.

## MULTIANODE GAS COUNTER

Multianode gas counter (MGC) consists of 5 plates (Fig. 1) which are printed-circuit boards made of FR4 with 0.5 mm width. The metal covering is 18 μm nickel, plated with 0.5 μm immersive gold.

Three central plates, which collect electrons of primary ionization at the middle anode in a quasi-uniform electrostatic field, form dual gap ionization chamber. This part of the detector allows to measure beam current in an ionization mode.

Lateral regions are proportional chambers for beam position and profile measurements. Electrons come to the anodes of a multichannel structure, which consists of 25 stripes with 100 μm width, 100 mm length and 4 mm spacing. Strong nonuniform field around stripes leads to electron avalanches, increasing the signal.
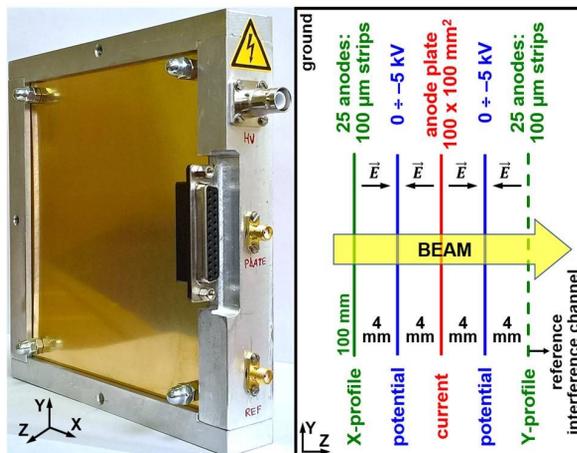


Figure 1: MGC photo and layout.

Modeling of this detector helps to find out operational characteristics of this counter, voltage range of power supplies and suitable gain of read-out electronics.

## IONIZATION CHAMBER

The filling gas is atmospheric air: 80% $N_2$ and 20% $O_2$ molecules at standard conditions. The amount of primary ionization electrons was calculated according to [1, 2], (Fig. 2).
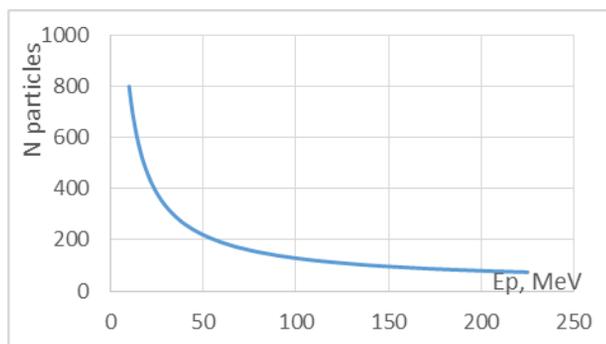


Figure 2: Number of primary electrons produced by an incident proton depending on its energy in the 4 mm gap.

Primary particles drift in the electric field undergoing various types of collisions with $N_2$ and $O_2$ molecules [3] (Fig. 3).
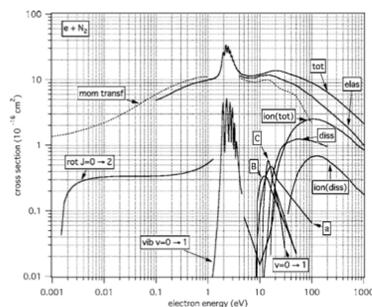
_____
† aleksey.melnikov@phystech.edu

Figure 3: Collision cross sections for $N_2$ molecule depending on incident electron energy [3].

The features of electron drift in a uniform field in the model were compared with Bolsig+ [4] calculations (Fig. 4). COMSOL model contains the same cross-section database as in the discussed program. The computed values of mean energy and Townsend coefficient are in a good agreement with Bolsig+ results.
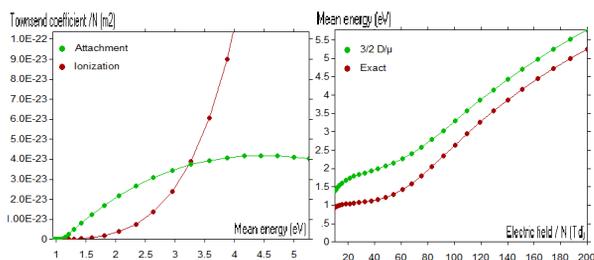


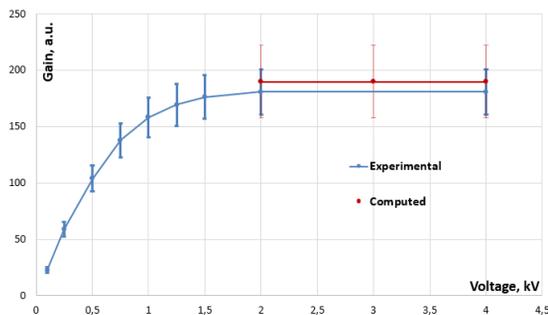Figure 4: Bolsig+ calculation results.



Figure 5: Experimental and computed total gain of MGC for 94 MeV proton energy in ionization chamber.

Model shows that about 30% of primary electrons disappear during a drift to the electrode because of attachment to $O_2$ molecules.

## PROPORTIONAL CHAMBER

Calculated electric field distribution around anode stripes (Fig. 6, 7) strongly depends on a stripe geometry. That is why information about detailed stripe shape after etching was needed.
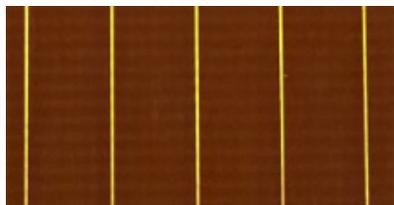


Figure 6: Photo of 100 μm stripes at the FR4 plate.

The approximate shape of a stripe (Fig. 7) was observed with the help of optical devices.
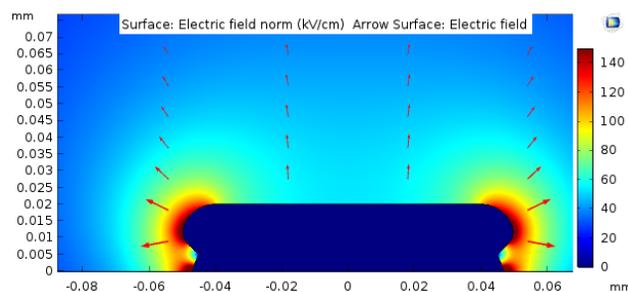


Figure 7: Distribution of electric field near a stripe at -4 kV potential.

Gain-voltage curve (Fig. 8) was calculated with the same gas processes as in the previous model.
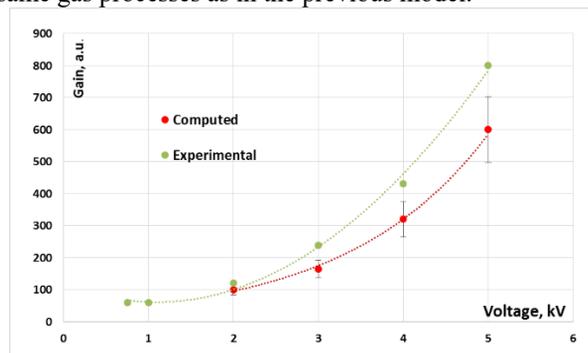


Figure 8: Experimental and computed gain-voltage curves for 94 MeV proton energy for proportional chamber.

In practice excitation cross-sections for $N_2$ and $O_2$ molecules are defined with 25 % accuracy in average [5], that defines the error of simulation.

## MGC IN USE

The front-end multichannel electronics of MGC operates with a conversion coefficient 45 mV/pC for each of 51 channels. The currents of secondary electrons are integrated over a pulse at each channel simultaneously and then signals are transmitted by a multiplexer with the processing time 24 μs per channel. The back-end electronics is NI USB-6003 DAQ module (ADC: 16-bit, 100 kS/s). The diagnostics software is based on LabVIEW and provides such options for MGC: data acquisition (Fig. 9), post processing, control of high-voltage supply and gain factor (1/10/100/1000) as well as a manual procedure of calibration by BCT.

The sequence of transmitted MGC signals is the following: beam signal from two central x and y profile stripes inside time integration gate, X and Y profiles and current signal. The maximum output voltage of ADC is 10 V (current signal is saturated on Fig. 9). Changing applied voltage is necessary to find the plateau of ionization region (Fig. 5). One can also disable voltage supply remotely while working with intensive beams measured by BCT in order not to damage the stripes.

The BCT signal (Fig. 9) is used for MGC calibration. Pulse duration data is also available. The result of

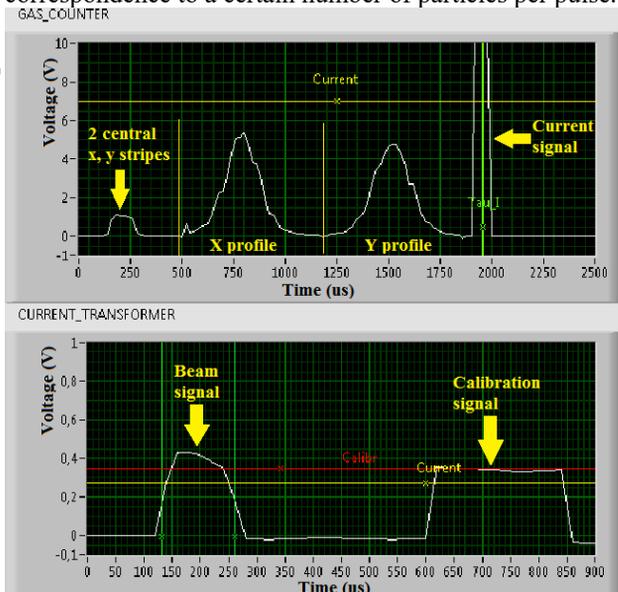calibration by BCT is MGC current signal (V) correspondence to a certain number of particles per pulse.



Figure 9: Signals from MGC and BCT.

Stripe spacing (4 mm) and ADC digitalization frequency (100 kS/s) mainly define resolution of the MGC profile signal. The procedure of calibration contributes to the main error in current measurements by MGC. In practice this relative error is about 10%.

## OPERATION FEATURES

The experimental operational range of MGC is $10^7 \div 10^{11}$ p/pulse with pulse duration about 130 μs.

It was found out that using intensive beams (with density $>10^{10}$ p/cm$^2$) leads to oxidation of MGC stripes. Temper colors are visible on Fig. 10. Oxide film (Fig.10) blocks low energetic electrons and decreases the signal. The way to solve the problem is to use O$_2$-free gas fill.

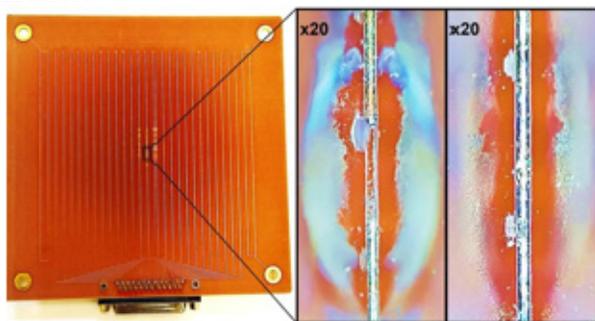Usage of beams less intensive than $10^7$ p/pulse decreases the signal below the MGC electronics threshold.



Figure 10: Aging effects at MGC strips: total and partial destruction.

Also it was noticed in the experiment that proton beams with incident energy < 20 MeV do not reach the last air gap of the counter. The way to solve this problem is to use thinner material along a beam path.

TRIM calculations confirm these experimental observations (Fig. 11).
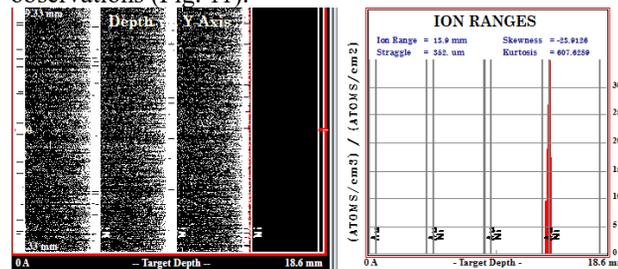


Figure 11: Range of 20 MeV protons in MGC volume.

## CONCLUSION

Beam diagnostic system consisting of MGC and BCT at the INR RAS linac was discussed. Detailed calculations of the detector response including particle tracing with gas processes in electric fields are presented. Simulated results, based on finite element model in COMSOL Multiphysics, are in a good agreement with experimental measurements.

The operational range of MGC was defined during the experiment – $10^7 \div 10^{11}$ p/pulse with pulse duration about 130 μs.

TRIM calculations confirmed the problem of radiation thickness at low energies.

Development of a new MGC with O$_2$-free gas fill is needed to prevent stripe destruction.

## REFERENCES

[1] NIST. stopping power and range tables for protons in various materials.

[2] G. Charpak, F. Sauli, "Multiwire Proportional Chambers and Drift Chambers", CERN, Geneva. Switzerland (1979).

[3] *Biagi database*, www.lxcat.net, copyright 2010.

[4] G.J.M. Hagelaar and L.C. Pitchford, "Solving the Boltzmann equation to obtain electron transport coefficients and rate coefficients for fluid models", Plasma Sci Sources and Tech 14, 722 (2005).

[5] D. C. Cartwright, "Electron impact excitation of the electronic states of N2", Physical Review, vol. 16, num.3.